Positron Annihilation in Phase-Separated $BaO\text{-}SiO_2$ Glasses

EDGAR DUTRA ZANOTTO*

Universidade Federal de São Carlos, 13560–São Carlos–SP Brazil

The kinetics of amorphous phase separation in $BaO\text{-}SiO_2$ glasses was studied by small-angle X-ray scattering and positron annihilation. Results show that the annihilation of positrons depends primarily on the average composition of the glasses; it therefore does not depend on compositional fluctuations caused by phase separation and cannot be used to determine the kinetics of phase separation in glasses.

INTRODUCTION

THE phenomenon of amorphous phase separation in glasses has considerable scientific and commercial interest, and several review papers have been published on the subject. Craievich *et al.*[1] reviewed the state-of-art of phase-separation kinetics, emphasizing new statistical theories[2] for spinodal decomposition and relations between amorphous phase separation and the nucleation and growth of crystals in glasses.

The experimental methods most widely used to study phase-separation kinetics are transmission electron microscopy (TEM) and small-angle X-ray scattering (SAXS). The study of properties such as viscosity and chemical durability can furnish additional information.

Apart from SAXS and TEM, Hautojärvi *et al.*[3,4] suggested that positron annihilation could be used to determine the volume fraction of droplets in phase-separated glasses.

This communication examines the applicability of the positron annihilation technique in assessing the kinetics of phase separation in glasses. $BaO\text{-}SiO_2$ glasses were used because they were previously studied by Zanotto *et al.*[5] by SAXS, and their behavior with respect to development of amorphous phase separation on isothermal heat treatment is known.

EXPERIMENTAL PROCEDURE

The melting procedure and chemical analysis are given in Refs. 5 and 6. The three compositions used contained 27.0, 28.3, and 33.2 mol% BaO (denoted throughout as glasses 27.0, 28.3, and 33.2). After heat treatment at 743°±1°C for up to 13 h, specimens 5 by 5 by 1 mm were cut and ground flat with SiC.

When a positron is injected into a vitreous material (after a lifetime of 10^{-9} to 10^{-10} s), it decays with an electron of the surrounding medium into gamma quanta. The annihilation process can be associated directly with valence electrons, or with initial formation of a positronium atom, or with localization into defects. The total-lifetime spectrum arising from the different processes can be decomposed into several lifetime components, which may be assigned to the cases just given.[7]

Positron lifetime and Doppler-broadened annihilation line-shape measurements were conducted at room temperature using a fast-slow coincidence system and an ^{22}Na positron source. The lifetime spectra were first analyzed by using three free exponential components; the detailed procedure is given elsewhere.[8] Since the standard deviations of the intensity of the longer positron lifetime component, I_3, were large, another analysis was made by fixing the positron lifetime, τ_3, at 1000 ps. The data presented here are based on this second analysis.

The SAXS experiments and corrections are described in Refs. 5 and 6.

RESULTS AND DISCUSSION

The integrated SAXS intensity in reciprocal space, Q, is proportional to the volume fractions of the scattering particles and of the matrix, ϕ_1 and ϕ_2, respectively, and to the electronic density difference between the two phases, $\Delta\rho$, i.e.

$$Q \propto \phi_1 \phi_2 \Delta\rho^2 \qquad (1)$$

Any changes in composition or volume fraction of the two phases will produce changes in Q.

Figure 1 shows that Q increases up to 7 h for glass 28.3 and up to 2.5 h for glass 27.0. Therefore, it can be concluded that the phase-separation process reaches its final stage, i.e. constant volume fraction of droplets and equilibrium composition of the matrix, after these periods. The values of Q were zero for glass 33.2 because this glass did not undergo phase separation.

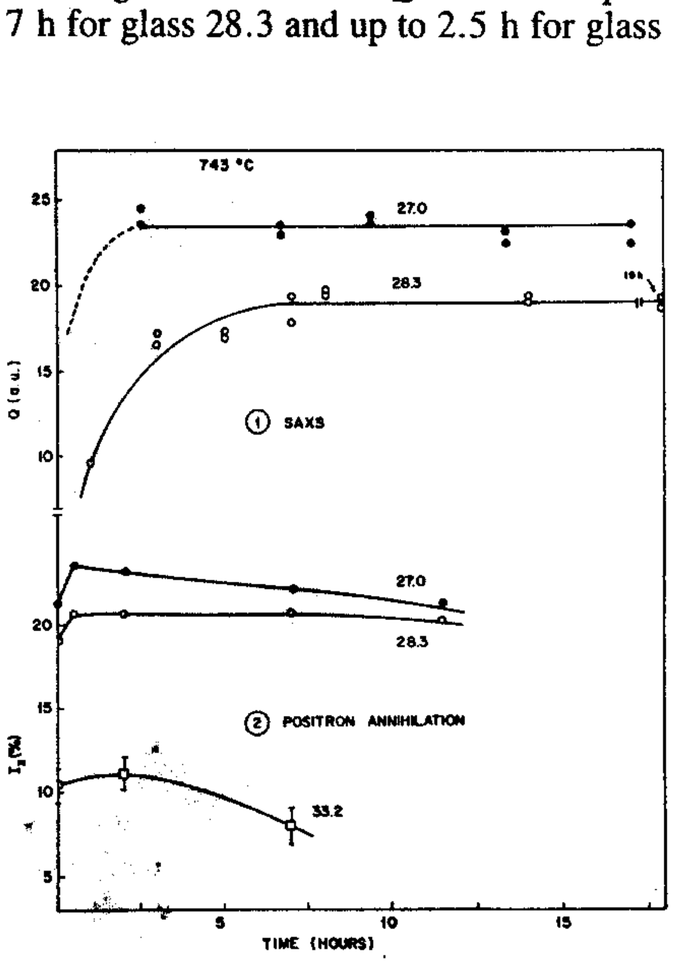

Fig. 1. (*Upper*) Integrated SAXS intensity and (*lower*) positron lifetime intensity as functions of heat-treatment time at 743°C (fixing τ_3=1000 ps).

Figure 1 also shows the intensity of the positron lifetime, I_3, as a function of heat-treatment time at 743°C. This intensity initially increases and then decreases slightly with time for both phase-separated (27.0 and 28.3) and homogeneous (33.2) glasses. This behavior cannot be readily explained because it occurs even in glass 33.2, which does not phase-separate and does not crystallize on heat treatment for up to 7 h at 743°C.[6]

The positron lifetime τ_3 is about the same, $\langle\tau_3\rangle$=1060 ps, for glasses 27.0 and 28.3, but it is remarkably smaller, $\langle\tau_3\rangle$=850 ps, for glass 33.2. The lifetimes τ_1 and τ_2 (Refs. 3 and 4) increased slightly, and the intensity I_2 decreased, with increasing BaO content; all these parameters were independent of time. These changes were, however, very small compared to changes in I_3.

In summary, it appears that there is no direct correlation between the SAXS and positron annihilation results shown in Fig. 1. The parameters I_3 and τ_3 show that the annihilation of positrons depends primarily on the mean BaO content of the glasses and not on the volume fraction of second phase. According to theory,[1] the volume fraction should vary as shown by the upper curves in Fig. 1, i.e. it should increase and become constant after a period of isothermal heat treatment.

CONCLUSION

Apparently the technique of positron annihilation does not correlate with the simpler results of SAXS and cannot be used in an obvious way to study the kinetics of amorphous phase separation. It depends primarily on the mean composition of the glass under study; i.e. the presence of submicroscopic compositional fluctuations do not substantially alter the annihilation of positrons. The small variation in positron annihilation with time of thermal treatment could be associated with the release of internal stresses in the glasses.

ACKNOWLEDGMENTS

The author acknowledges Prof. Pekka Hautojärvi of Helsinki University of Technology for performing the positron measurements and Dr. P. F. James of Sheffield University for critical review of the manuscript.

REFERENCES

[1] A. F. Craievich, E. D. Zanotto, and P. F. James, "Kinetics of Subliquidus Phase-Separation in Silicate and Borate Glasses. A Review"; to be published in *Bulletin de la Societe Francaise de Mineralogie et de Cristallographie*.

[2] A. F. Craievich and J. M. Sanchez, "Dynamical Scaling in the Glass System B_2O_3-PbO-Al_2O_3," *Phys. Rev. Lett.*, **47**, 1308–11 (1981).

[3] P. Hautojärvi, A. Vehanen, V. Komppa, and E. Pajanne, "Crystallization and Phase-Separation of $Li_2O\text{-}SiO_2$ Glass," *J. Non.-Cryst. Solids*, **29** [3] 365–81 (1978).

[4] P. Hautojärvi and E. Pajanne, "Positron Annihilation in Phase-Separated and Crystallized Silicate Glasses," *J. Phys. C.*, **7** [21] 3817–26 (1974).

[5] E. D. Zanotto, A. F. Craievich, and P. F. James, "SAXS and TEM Studies of Phase-Separation in $BaO\text{-}SiO_2$ Glasses"; Proceedings of the Fifth Symposium

CONTRIBUTING EDITOR—R. K. MACCRONE

Received November 1, 1982; approved November 12, 1982.

*Member, the American Ceramic Society.

on Physics of Non-Crystalline Solids, Montpellier, July 1982.

[6]E. D. Zanotto, "The Effects of Amorphous Phase Separation on Crystal Nucleation in Baria-Silica and Lithia-Silica Glasses"; Ph. D. Thesis, Sheffield University, 1982.

[7]R. N. West, "Positron Studies on Condensed Matter," *Adv. Phys.*, 22, 263–86 (1973).

[8]C. Dauwe, M. Dorikens, and L. Dorikens-Vanpraet, "Positron Annihilation in Solids"; Third International Conference on Positron Annihilation, Otaniemi, Finland, 1973. □

Static Fatigue of Silica in Hermetic Environments

J. A. WYSOCKI

Hughes Research Labs, Malibu, California 90265

Static fatigue tests on metal-coated silica fibers have shown subcritical crack growth with crack velocities ranging from $\approx 10^{-14}$ to 10^{-17} m·s^{-1}. To induce subcritical crack growth, however, it is necessary that the test be performed at stress intensities, K_I, of $>0.8\ K_{Ic}$. Metal-coated fibers provide a unique medium for studying static fatigue at these high stress levels because the metal coating protects the fiber from the external environment. Crack growth for these tests demonstrates the sensitivity of crack velocity to OH^- concentrations at the crack site.

IN THE fiber optics industry, interest concerning the static, or dynamic, fatigue of optical fibers centers on accurate prediction of fatigue lifetimes based on available laboratory data. Although it is generally agreed that static fatigue represents a decrease in strength caused by stress-enhanced corrosion of pre-existing flaws in the silica by water, accurate failure predictions cannot be made because of insufficient quantitative information on the factors affecting static fatigue. Attempts to fit experimental data to a general crack-velocity equation have demonstrated success with four forms of the equation.[1] Generally, all four forms converge in the region of experimental results; they are, however, divergent outside this region.[1]

Although the influence of temperature, humidity, chemical acidity, loading rate, and stress on static fatigue behavior has been addressed,[2,3] little is known about fatigue behavior in hermetic environments or at very slow crack-growth velocities ($<10^{-13}$ m·s^{-1}). Since knowledge of static fatigue behavior in these regimes would be useful for lifetime predictions, a series of static fatigue tests was conducted. Metal-coated fibers were utilized for these tests since metal coatings provide the fiber with a hermetic jacket[4]; consequently, tests that were independent of external environment could be conducted.

However, even commercial optical waveguide fibers are known to have OH^- impurities exceeding ≈ 100 ppm. This OH^- content is considered to be sufficiently high to trigger subcritical crack growth, even in hermetic environments, when the critical stress intensity is sufficiently high and the loading time sufficiently long. Wiederhorn[5] has shown for borosilicate glasses, that crack velocity is related to stress intensity at the crack tip and that the velocity can be varied by controlling the amount of moisture in the environment.

In previous investigations, metal-coated fibers were shown to be insensitive to both static[4] and dynamic[6] fatigue, presumably because the stress intensity level of those tests was not high enough to induce subcritical crack growth for the amount of OH^- present. Consequently, in the present investigation four sets of metal-coated fibers, each with different mean strengths, were prepared. In this way, the fiber could be stressed to >80% of its critical stress at different test stress levels. As a result, static fatigue behavior in terms of both relative stress and absolute stress was obtained.

Each set of fibers was wrapped on a mandrel to induce a stress proportional to the fiber diameter and the mandrel diameter, as given by:

$$\sigma_a = (d/D)E \qquad (1)$$

where σ_a is the effective tensile stress, d the fiber diameter, D the mandrel diameter (including the diameter increase contributed by the metal jacket), and E Young's modulus for silica.[7] The composite failure time versus the failure-probability distribution is shown in Fig. 1. The failure probability is taken, as in the Weibull distribution, to be $1/(a+1)$, where a is the total number of samples tested.

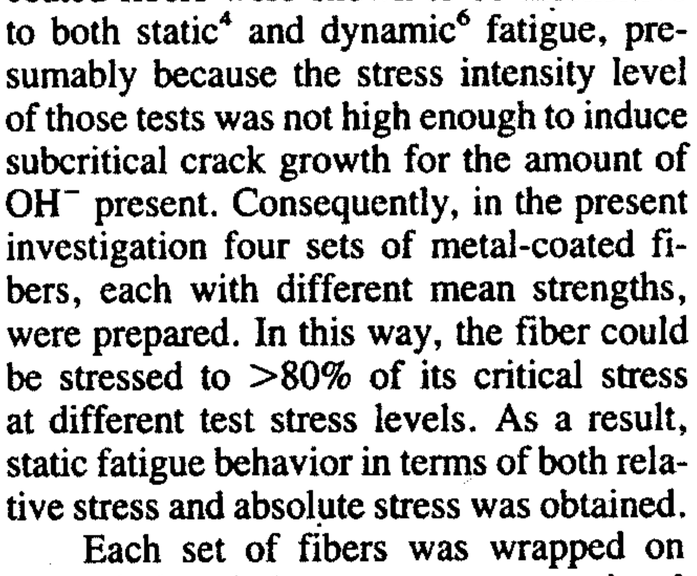

Fig. 1. Failure times plotted as a function of survival probability for sets of metal-coated fibers tested at four stress levels.

The characteristic strength distribution for each set of metal-coated silica fibers was obtained by using samples 0.5 m long tested in tension at a strain rate of 0.2 min^{-1} to construct a Weibull distribution. Each Weibull distribution was then fitted to a straight line using linear regression analysis. However, since the distribution is constructed with sample lengths different from the lengths used in the actual static fatigue tests, it is necessary to transform the data by $\ln S(L_1/L_0)$, where S is the survival probability defined as $(1\text{-}F)^{-1}$ and (L_1/L_0) is the ratio of the mandrel sample length (L_1) to the length of the sample tested in tension (L_0). This transformation is used to describe the slope and intercepts of the actual sample length used in each test. Because the fiber must survive the stress induced by wrapping it on the mandrel, each static fatigue test can be considered an in-situ proof test; the distribution is considered to be attenuated and is further modified so that the failure probability, P_a, is:

$$P_a = P_i - P_p/(1-P_p) \qquad (2)$$

where P_i is the initial failure probability and P_p the failure probability at the proof stress.[8] This Weibull distribution is used to describe the expected mechanical behavior of the samples used in the static fatigue tests (Fig. 2).

Wilkins' technique of homologous strength,[9] which allows calculation of the initial flaw size from a failed sample when the initial stress versus probability distribution is known, is then applied to the data shown in Figs. 1 and 2. For each static fatigue failure, as shown in Fig. 1, a failure probability is assigned. Each datum point is then superimposed on the appropriate failure distribution in Fig. 2, so that for each failure probability, a corresponding initial stress can be determined. These initial stress values are then normalized by σ_a, the mandrel test stress, to obtain the homologous stress, σ_H, which is plotted in Fig. 3 as a function of the original corresponding failure times from Fig. 1. The failure time versus homologous stress data in Fig. 3 then becomes the basis for a K_I-V diagram since

$$K_{Ii} = (\sigma_a/\sigma_{Ic})K_{Ic} \qquad (3)$$

as shown by Wiederhorn,[2] where K_{Ii} is taken to be the initial stress intensity, σ_a is the maximum stress applied by the mandrel test (Eq. 1), σ_{Ic} is the critical fracture stress in an inert environment (Fig. 2), and K_{Ic} is a material constant for silica taken to be 0.75 MPa·m$^{1/2}$ (Ref. 2). It follows that

$$K_{Ii} = \sigma_H K_{Ic} \qquad (4)$$

The right side of Fig. 3 is shown as K_I in units of MPa·m$^{1/2}$ to reflect this relation.

CONTRIBUTING EDITOR — A. G. EVANS

Received February 2, 1982; revised copy received November 18, 1982; approved December 13, 1982.